

Machine learning applied to functionalized graphene sensors for noninvasive detection of renal diseases

Sarkar, Lisa; Bhattacharyya, Arindam; Sett, Avik; Karmakar, Gairik; Bhattacharyya, Tarun Kanti

DOI

[10.1109/BIBM62325.2024.10822275](https://doi.org/10.1109/BIBM62325.2024.10822275)

Publication date

2024

Document Version

Final published version

Published in

Proceedings - 2024 IEEE International Conference on Bioinformatics and Biomedicine, BIBM 2024

Citation (APA)

Sarkar, L., Bhattacharyya, A., Sett, A., Karmakar, G., & Bhattacharyya, T. K. (2024). Machine learning applied to functionalized graphene sensors for noninvasive detection of renal diseases. In M. Cannataro, H. Zheng, L. Gao, J. Cheng, J. L. de Miranda, E. Zumpano, X. Hu, Y.-R. Cho, & T. Park (Eds.), *Proceedings - 2024 IEEE International Conference on Bioinformatics and Biomedicine, BIBM 2024* (pp. 6138-6144). (Proceedings - 2024 IEEE International Conference on Bioinformatics and Biomedicine, BIBM 2024). IEEE. <https://doi.org/10.1109/BIBM62325.2024.10822275>

Important note

To cite this publication, please use the final published version (if applicable).

Please check the document version above.

Copyright

Other than for strictly personal use, it is not permitted to download, forward or distribute the text or part of it, without the consent of the author(s) and/or copyright holder(s), unless the work is under an open content license such as Creative Commons.

Takedown policy

Please contact us and provide details if you believe this document breaches copyrights.
We will remove access to the work immediately and investigate your claim.

Green Open Access added to TU Delft Institutional Repository

'You share, we take care!' - Taverne project

<https://www.openaccess.nl/en/you-share-we-take-care>

Otherwise as indicated in the copyright section: the publisher is the copyright holder of this work and the author uses the Dutch legislation to make this work public.

Machine learning applied to functionalized graphene sensors for noninvasive detection of renal diseases

Dr. Lisa Sarkar
*Department. of Electronics and Electrical Communication engineering
 IIT Kharagpur
 Kharagpur, India
 lisasarkar11@gmail.com*

Gairik Karmakar
*Department. of Electronics and Electrical Communication engineering
 IIT Kharagpur
 Kharagpur, India
 karmakar.gairik@gmail.com*

Arindam Bhattacharyya
*Department of Computer and Electrical Engineering
 UC Davis
 line 5: abhattacharyya@ucdavis.edu*

Prof. Tarun Kanti Bhattacharyya
*Department. of Electronics and Electrical Communication engineering
 IIT Kharagpur
 Kharagpur, India
 tkb@ece.iitkgp.ac.in*

Dr. Avik Sett
*Department. of Microelectronics
 TU Delft
 Delft, Netherlands
 settavik.research@gmail.com*

Abstract— Breath biomarker detection has been a significant non-invasive approach for disease diagnosis. This method has significant potential for early diagnosis and accurate analysis of diseases. Emission from breath contains several volatile organic compounds. Among them, ammonia is a very commonly found VOC and mainly responsible for chronic kidney diseases. There exist several strategies to detect ammonia, however they demonstrate severe limitations such as cross-sensitivity and poor selectivity. This work demonstrates the synergistic effect of sensor functionalization and application of machine learning for selective detection of ammonia in the environment. The sensor exhibits high degree of selectivity towards ammonia owing to enormous hydroxyl groups contributed through curcumin. At 500 ppm ammonia, the sensor demonstrates 274% response and very high selectivity among seven volatile organic compounds. The machine learning models were trained with the help of sensor transients. Random Forest and CNN models were applied to predict the presence of ammonia in a mixture. Random Forest achieved 96.25% accuracy compared to 89% accuracy of CNN. Hence, Random Forest algorithms applied to curcumin functionalized reduced graphene oxide sensors can detect ammonia vapors with very high efficiency among a mixture of gases.

Keywords— *Ammonia Sensor, Reduced graphene oxide, Curcumin, Random Forest, Convolutional neural network*

I. INTRODUCTION

Air quality monitoring is highly essential due to an explosion in chemical, food and automobile industry. Highly selective and sensitive gas sensors are the backbone of air quality monitoring systems. The main attributes of a gas sensor includes operation at minimum power, room temperature and high specificity. In this context, several nanomaterials such as ZnO, Fe₂O₃, WO₃, SnO₂, are explored [1-3]. These semiconductor metal oxide nanostructures are highly efficient in sensing organic and inorganic gases. However, they typically need very high temperatures (150–400 °C). for their optimum operation. Cross-sensitivity to other gases except the target analyte is also a primary concern for these type of sensing materials. High operating temperature and large power requirements limits their application in many wireless, flexible and hand-held

devices.

Metal oxide-based Taguchi sensors that are available commercially operate at 200 mW power rating. Moreover, these sensors suffer sensitivity issues in presence of humidity and other toxic gases.

Therefore, there is a pressing need to develop gas sensors that operate at room temperature and are highly selective towards a particular gas eliminating the cross-interferences. An approach of functionalization of nanomaterials is identified by the researchers. Here, specific functional moieties are attached to the sensing nanomaterial to impart high degree of selectivity. The approach of functionalization not only benefits from high selectivity but also imparts high sensitivity and quick response. The high surface to volume ratio of two-dimensional nanomaterials have gained wide attention for appropriate functionalization. Graphene, black phosphorus, molybdenum di-sulfide, tungsten di-sulfide are excellent candidates for fabricating functionalized gas sensors with high efficiency. The room temperature operation of these materials are highly beneficial as the ignition temperatures of certain toxic gases like ammonia and hydrogen disulfide is low.

Graphene has attracted wide attention owing to very high surface area, high mobility, thermal and mechanical stability, flexibility and ease in functionalization. The high surface to volume ratio ensures most of the atoms are at the surface. This leads to very high sensitivity to environmental perturbations. Graphene exhibits very high response and sensitivity due to 2D honeycomb structure and atomically thin layer. Graphene in its pure state is free from defects which imparts extremely small adsorption energy towards various gases and analytes. Generation of defect states and doping in graphene increases the adsorption energy through charge transfer, which leads to increase in specificity towards different analytes. A form of graphene, known as graphene oxide (GO) is a chemically oxidized form of graphene. The oxidation of graphene sheets allows ease in exfoliation and separation of graphene layers. In the oxidized form, GO is not a good candidate for sensor applications due to its insulating nature and low immunity towards humidity. When this form of graphene (GO) is

reduced, the oxygen species attached to graphene sheet vanishes to a certain extent. The graphene backbone is then partially restored with added functionality. Moreover, during reduction, various reducing agents with specific functional moieties are utilized to covalently functionalize graphene sheets. The increased mobility of the reduced graphene oxide (rGO) sheets along with sufficient functional groups and defects can now be an excellent candidate for gas sensing applications at room temperature.

Ammonia is a very toxic and pungent gas used in many industries as common reagent. The presence of ammonia in air causes adverse respiratory diseases and also affects the skin and eyes when exposed at concentration greater than 400 ppm [4]. When exposed to very high levels of ammonia (several thousand ppm), complicated health issues arises leading to death. As designated by OSHA (Occupational safety and health administration), 15-28% of ammonia concentration by volume is severe to human lives [5]. Moreover, ammonia being flammable, demands design of sensors that can operate at room temperature. Few graphene based devices have been reported for detection of ammonia [6-8], however their poor recoverability, baseline drift and cross-sensitive nature limits their use in most applications. The previous research works leaves sufficient gaps in analysis of sensor response in a mixture of gas. With proper application of machine learning algorithms to functionalized graphene based sensors, an efficient sensing performance is expected to be achieved [9,10].

Electronic nose (E-nose) is a device that is used to detect specific gases for medical, environmental and industrial applications. It usually couples a sensor array with some processing algorithms to track the presence of a gas. Most of the gas sensor arrays uses a set of sensor to detect one single gas. This research work expands this concept to detect ammonia in presence of several gases with the help of deep learning (DL) algorithms applied to a functionalized graphene sensor. The proposed system minimizes consumption of power by applying DL algorithm to a single sensor. The DL algorithm is highly robust to even classify noisy data sets. In this work, ammonia concentration is predicted in presence of other interfering gases. A single functionalized sensor is used along with Random Forest and Convolutional neural network (CNN) for classification. Every class is denoted with separate range of gas mixture concentration, where the ammonia levels are varied. The use of a single functionalized sensor and classification in a mixture can build up high performing sensor systems for air quality monitoring.

II. STATE OF THE ART

In a research based on graphene field effect transistor, the authors coupled multi-layer perceptron to develop an electronic nose [11]. The conductance of the graphene FET was analyzed and a 4D space was used to project the physical properties. Mobility of electrons, mobility of holes, concentration of carrier were used as features. The feature domain was expanded by addition of ruthenium dioxide to the graphene FET. The system was designed to detect ethanol, methanol and water. An accuracy of 96.2% was achieved. However, the gases was tested individually, which is very different from the actual scenario where multiple gases may be present.

In another work, eight sensors was used to fabricate a sensor array. The sensors data trained a CNN algorithm which was used to discriminate four test gases. The selected gases were methane, hydrogen, carbon monoxide and ethylene [12]. The training dataset was applied to support vector machine. However, the highest accuracy of 95.2% was obtained on application of CNN on the sensor array.

The authors of [13] developed a sensor system comprising eight sensors. They coupled the sensor data to CNN. Here, sensor data was collected as images. Data preprocessing and images fed to CNN was used to discriminate different gases. The accuracy of such a system was close to 94%.

Another research group [14] developed a system based on electronic nose using eight sensors. They coupled their sensor data to decision tree algorithm and targeted five gases. Carbon monoxide, carbon dioxide, hydrogen, propane and ammonia was used for testing and validation.

The research group in [15] utilized MOSFET based sensor array and artificial neural network to boost the selectivity of a gas sensor array. The sensor was tested in two specific gas mixture specifications. One such mixture comprised of ammonia, hydrogen and ethanol, and the other had hydrogen, air and acetone.

III. FABRICATION OF FUNCTIONALIZED SENSOR DEVICE

A $p<100>$ oriented silicon wafer having a resistivity of 4-20 $\Omega\text{-cm}$ was used as a substrate. The silicon wafer was oxidized thermally to grow a 200 nm silicon dioxide insulation layer over the substrate. Prior to gold deposition, 20 nm chromium was deposited as an adhesive layer. Chromium layer deposition followed by 200 nm gold deposition was carried out by DC sputtering. The electrodes were patterned photolithographically in an interdigitated manner. The fingers of the interdigit was separated by 50 μm . The gaps were filled by depositing functionalized graphene solution over the electrodes. Room temperature drying completed the formation of the sensor devices. The sensing material formed the channel of the device. Curcumin was used to reduce graphene oxide and at the same time was used to functionalize the graphene sheets. The schematic of the sensor device containing the functionalized sensing layer and electrodes are depicted in figure 1.

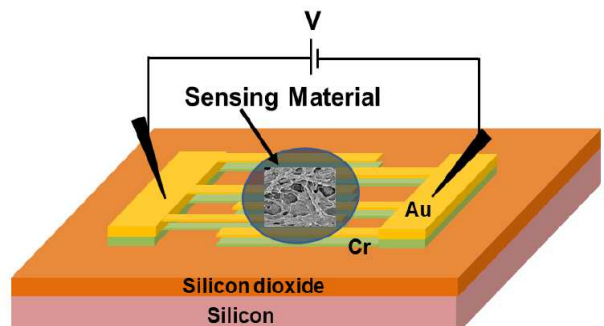


Figure 1. Schematic of functionalized graphene sensor

Chemical exfoliation of graphene sheets were carried out for preparation of graphene oxide. Hummer's method was used to synthesize the graphene nanosheets. Graphite powder was mixed with sodium nitrate and stirred for 8 hours in sulfuric acid. The solution was then brought to 0 $^{\circ}\text{C}$

with the help of ice bath. Potassium permanganate was added in very minute quantities while stirring. The temperature was maintained below 12 °C. After completion of mixing, the solution was brought to room temperature with the help of hot plate. Addition of DI water to initiate an exothermic reaction was carried out. The temperature of the solution raises to 98 °C and after half an hour the reaction is forcefully inhibited by placing the beaker in a water bath. The solution turns blackish from its inherent brown colour. After an hour, DI water is added followed by addition of hydrogen peroxide. This turns the solution bright yellow. This change in colour signifies successful formation of graphene oxide (GO). The solution was washed several times to ensure a pH of 7. The GO sheets were further subjected to high power ultrasonication for more exfoliation.

Curcumin was used for simultaneous reduction and functionalization. Ethanol was used to dissolve curcumin (10 mg in 20 ml ethanol). The solution was stirred for a hour and then added to GO while stirring vigorously. The pH of the mixture was maintained at 10 by addition of ammonia solution during stirring process. The mixture was then transferred to a red capped reagent bottle and heated at 95 °C for 3 hours. The solution was further cooled down and the resulting sensing solution was named cf-rGO.

IV. SENSOR LAYER CHARACTERIZATION

The fabricated sensor layer was characterized through structural, morphological study and compositional analysis. FESEM, HRTEM, XRD, FTIR and RAMAN spectroscopy was conducted to analyze the physical and chemical properties of the sensing layer. The structural characterization of cf-rGO shows wrinkled sheet like structures in FESEM images as depicted in figure 2(a). Defects are the adsorption sites for such sheet like structures. The presence of wrinkles demonstrates functional defects created on the graphene sheets. More evidence is visible from HRTEM images of the cf-rGO layer. Figure 2(b) demonstrates the HRTEM images of the as prepared sensing layer.

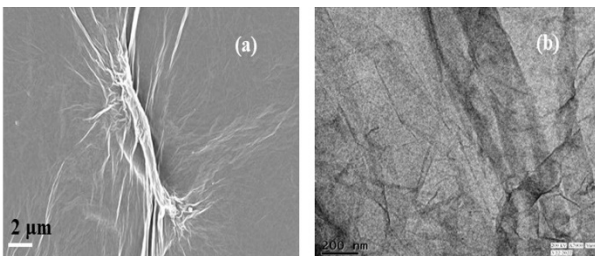


Figure 2. (a) FESEM image of Cf-rGO nanosheets (b) HRTEM image of Cf-rGO nanosheet

The structural analysis was carried out through X-ray diffraction. The radiation of Cu K α 1 ($\lambda = 1.54 \text{ \AA}$) was used along with a parallel beam diffractometer. Figure 3(a) shows the XRD analysis of GO and cf-rGO sensing materials. A sharp peak at 10.48° was observed for GO which is due to reflection from the (001) plane. Successful reduction of GO to cf-rGO is visible from the broad peak centred around 24.57°. This peak arises from the (002) plane of the cf-rGO sheets.

The FTIR spectra for GO and cf-rGO is depicted in figure 3(b). The O-H group vibrations are observed as broad peak

at 3000-3500 cm^{-1} [16]. The carboxylic groups (C=O) are generally present near the sheet edges, are evident in the spectra at 1740 cm^{-1} . There are several functional groups present in the GO sheet. The peaks at 1048 cm^{-1} , 1220 cm^{-1} and 1373 cm^{-1} accounts for C-O stretching, C-O-C stretching and C-OH stretching respectively [16-17]. These functional groups are eliminated when the GO is subjected to reduction with the help of curcumin. The successful reduction of the GO sheet is evident from the spectra in figure 3(b). Apart from the hydroxyl groups, the other groups are observed to vanish after reduction. The presence of hydroxyl groups is very significant as it binds to ammonia molecules with higher adsorption energy. Such specific functionalization has severe benefits for selective detection of target gas molecules.

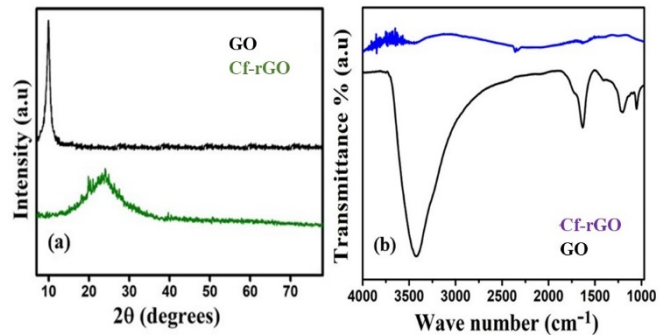


Figure 3. (a) XRD analysis of GO and Cf-rGO and (b) FTIR spectra for GO and Cf-rGO

The simultaneous functionalization and reduction of GO to form cf-rGO can be further validated with the help of Raman analysis. The Raman spectra for GO and cf-rGO is elucidated in figure 4(a) and 4(b) respectively. The D and G band of graphene oxide (GO) is observed at 1366 cm^{-1} and 1607 cm^{-1} respectively [18]. The successful reduction of the graphene oxide sheets is accomplished with a left shift in the Raman spectra. The D and G bands of the cf-rGO was observed at 1357 cm^{-1} and 1599 cm^{-1} respectively, which is the signature that graphene oxide is successfully reduced [19]. Attachment of curcumin molecules with the unsaturated carbon atoms results in the shift of D and G bands in the Raman spectra. Curcumin being a reducing agent, donates electrons to the GO sheet, resulting in softening of phonons during the interaction [20-21].

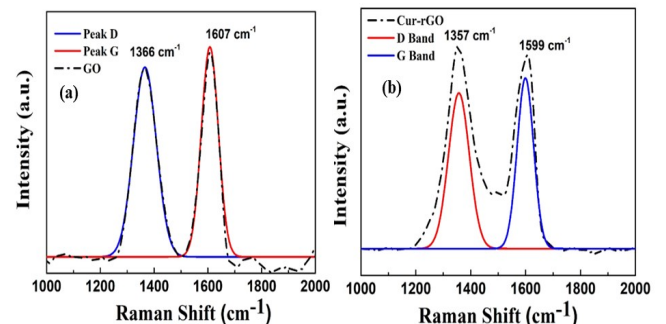


Figure 4. (a) Raman analysis for GO (b) Raman spectra for Cf-rGO

V. SENSING MECHANISM AND RESULTS

Functionalization of curcumin onto the graphene sheets was done during the reduction process. The prepared curcumin functionalized reduced graphene oxide sheet is abbreviated

as cf-rGO. The cf-rGO sensing layer exhibited a p-type sensing characteristics. Pure graphene sheets that are defectless are often associated with very low adsorption energies. When graphene sheets come in contact with ammonia molecules, the adsorption energy is calculated to be 0.114 eV [22]. For sensing applications, the graphene sheets must be induced with several defect sites to increase the adsorption energy towards a particular gas. This is achieved through proper functionalization. When hydroxyl and epoxy groups are attached to graphene sheets, the adsorption energy towards nitrogen containing molecules were found to be 0.84 eV and 0.219 eV respectively [22]. Hence, with proper functionalization, the adsorption energy and hence the sensitivity can be increased.

The exposure of cf-rGO to ammonia molecules, lead to charge transfer from the ammonia molecules to the hydroxyl groups of cf-rGO sensing layer. Ammonia behaves as Lewis base and efficiently transfers electron to the cf-rGO sheets. These electrons recombine with the majority holes of the cf-rGO and reduces the conductivity of the device. The highly efficient functionalization leads to significant increase in adsorption energy, given as:

$$E_b = E_{\text{slab}} + E_{\text{mole}} - E_{\text{mole+slab}} \quad (1)$$

where, E_{slab} is represented as the energy of the graphene surface, E_{mole} is energy of the ammonia molecules and $E_{\text{mole+slab}}$ is the energy of the system comprising gas-graphene interface and ammonia vapors.

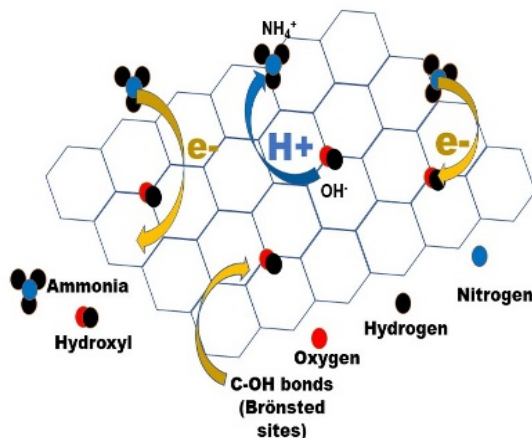


Figure. 5 Schematic of sensing mechanism for cf-rGO

The charge transfer takes place through two possible mechanisms as elucidated in figure 5. Firstly, the ammonia molecules, acting as Lewis base, transfers electron to the p-type graphene matrix. This reduces the hole concentration in the cf-rGO sheet leading to increase in resistance. Secondly, the C-OH functionalization over the cf-rGO sheet acts as Brønsted sites and donates proton to the incoming ammonia molecules. The decrease in positive charge from the cf-rGO sheets also induces increase in resistance. The combination of these two mechanisms lead to overall increase in sensor resistance. The change in resistance is calibrated as sensor response for different concentration of ammonia vapors.

The repeatability of the sensor was tested when it was exposed repeatedly to 500 ppm ammonia concentration. The repeatability test was conducted four times as shown in

figure 6(a). During exposure to 500 ppm ammonia, the cf-rGO based sensor exhibited a response time of 53 seconds. The recovery time was found to be 38 seconds. The cf-rGO sensor showed a very good recoverability with almost zero baseline drift. High efficiency of the sensor including fast recovery and response can be attributed to curcumin functionalization of the rGO sheets. The specific hydroxyl groups not only facilitates efficient charge transfer but also ensures easy release of ammonia vapors during recovery cycle. Selectivity is a very significant attribute of a sensor which was evaluated in presence of seven VOCs. Ammonia, acetone, toluene, benzene, methanol and ethanol were used to test the sensor's specificity. The sensor demonstrated very high selectivity towards ammonia vapors, but also showed little response towards toluene, acetone and formaldehyde. Machine learning algorithms such as CNN and Random Forest models play a pivotal role in detecting ammonia in presence of these three gases. The selectivity of the cf-rGO sensor is demonstrated in figure 6(b).

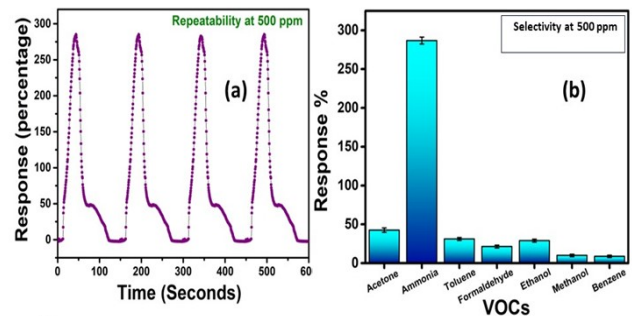


Figure. 6 (a) Repeatability of cf-rGO at 500 ppm ammonia and (b) Selectivity of cf-rGO in presence of seven VOCs

The sensor exhibited a quick response time of 23 seconds and decent recovery time of 71 seconds when exposed to 250 ppm ammonia concentration. Commercial gas sensors have a tendency to show response fluctuations in presence of humidity. Previously reported graphene sensors have suffered humidity sensitiveness to a great extent. Thereby, cf-rGO based sensor was subjected to different levels of humidity to analyze the response deviations. As demonstrated in figure 7(a), the sensor showed strong immunity towards humidity till RH value of 80%. The sensor demonstrated around 6% deviation when the RH levels crossed 90%. The sensor was tested for stability with 500 ppm ammonia concentration. The test was carried out for 50 days. The promising results signifies the potential use of the cf-rGO sensor for air quality monitoring.

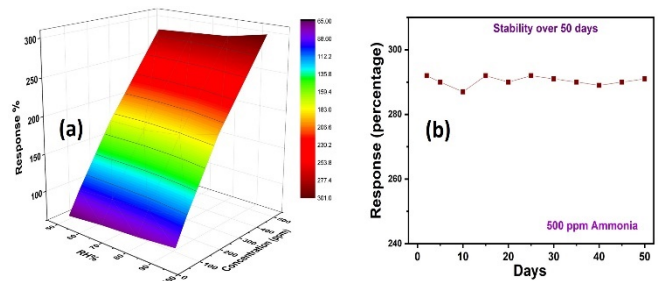


Figure 7. (a) Response vs humidity plot and (b) Stability plot

Different mixtures of gases were made to expose the sensor to different environments. The evaluation of response in cross-sensitive environments is vital for accurate detection of gases. Machine learning algorithms was applied to the derived response of the cf-rGO sensor towards these various mixtures. Three mass flow controllers (MFC) was used to create different gaseous environments. One dedicated MFC was used to flow different concentration of ammonia, and the other two MFCs were used to flow either of toluene-acetone, toluene-formaldehyde or acetone-formaldehyde in different concentrations. The combinations of these four gases created a dataset for training the machine learning/deep learning models. The created gaseous environments and the use of deep learning (DL) to a sensitive cf-rGO layer provides a highly accurate gas detection strategy in a mixture of gas.

The transient response of the sensor was collected for different gas mixtures and ammonia was intended to be the target gas. The transient response was collected by exposing the sensor to the differently created environment, and the current level was traced with respect to time at a constant applied voltage. For a single gas scenario, ammonia, toluene, formaldehyde and acetone was exposed to the cf-rGO sensor separately at 50, 100, 250 and 500 ppm concentrations.

In the scenario where two gases are present, with ammonia as target gas, one of the three gases was mixed with ammonia to create the mixture. (Ammonia + Toluene), (Ammonia + Acetone) and (Ammonia + Formaldehyde) with different concentration was formulated and cf-rGO was exposed to these gas mixtures. The transient responses from this binary system were collected to train the deep learning models.

Furthermore, ternary gaseous environments were created by mixing ammonia with two of the three gases at separate concentrations. (Ammonia + Toluene + Formaldehyde), (Ammonia + Acetone + Toluene) and (Ammonia + Acetone + Formaldehyde) were used to create the three-gas mixture scenario. The transients were collected for individual mixtures with specific concentration ratios and applied to the DL models.

Through this method, the data was collected for 31 classes of gas mixtures. In one segment, ammonia concentration was kept constant and the other gas concentrations were varied. In another segment, other gas concentrations were kept constant and ammonia concentration was varied. Deep learning models were trained for these different classes and then tested for validation.

A. Data modification

In the collected transient response from the sensor, the data contained current level changes with respect to time. The efficiency of the deep learning model was enhanced by converting the mono-variate time series data to multi-variate time series. This is done by addition of saturation and recovery time, saturation and recovery current levels and total gas mixture concentrations. The individual mixture classes were segregated into recovery and saturation regimes. The saturation parameter in the saturation regime is

set according to equation 1 and 2. The saturation parameter is set to zero in the recovery regime. Similarly, recovery is set to zero in the saturation regime and recovery parameters in the recovery zone is expressed by equation 3 and 4.

rec[*t*]=0.....(2)

B. CNN

In a complex gaseous environment, ammonia concentration is predicted using convolutional neural network or CNN. The application of CNN is described as follows:

Initially, there is one input layer with a 32 filter, a convolution layer (three kernel) and an activation layer along with a normalization layer. Moreover, there are additional three convolution blocks associated with 64 filter each. These blocks also comprise 3 kernel convolution layer, activation layer and normalization stage. There is a third convolution block with 64 filters. There is an additional three convolution block each with 128 filter, 3 kernel convolution layer, activation layer and normalization stage. An average pooling block is connected to the final block and this connects to the output layer through a dense system. Overall, 25 layers are used in the CNN model. Prevention of over-fitting is done by an Adam optimizer.

C. Random forest

Random Forest model is a machine learning technique where multiple classification algorithms are used. The final layers declares the class that received maximum vote as the output. Random Forest can be viewed as collection of decision trees, which selects the output class that receives the maximum votes. Random Forest is a hierarchical body with leaves, branches and nodes. The available features are used to construct the decision node, then the process is moved to the output leaf or the next node [23]. In this work, decision tree with 100-nodes is used to perform the detection of ammonia vapor in a gas mixture environment.

D. Results

The transient data collected from the sensor was divided into 80-20 split, 80% being the training data set and the rest 20% being the validation data set. The training data set was fed to the CNN model for classification. In the training for CNN, the initial learning rate, stopping learning rate and reduction factor was chosen to be 0.001, 0.00001 and 75% respectively. The optimum batch size was chosen to be 64. Figure 8 demonstrates the 89% test accuracy including 0.27 loss factor. Figure 9 depicts the accuracy curve analyzing the loss in training and validation. The loss curve shows that

the model demonstrate a good fit to the data.

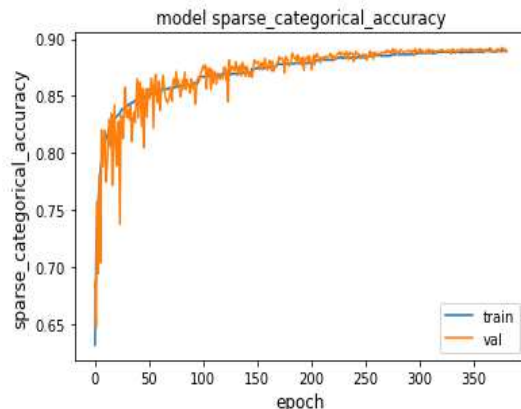


Figure 8: Training accuracy of CNN

The same data set was also used to train the random forest model. The accuracy achieved was 96%. Fifteen nodes were set for the random forest model.

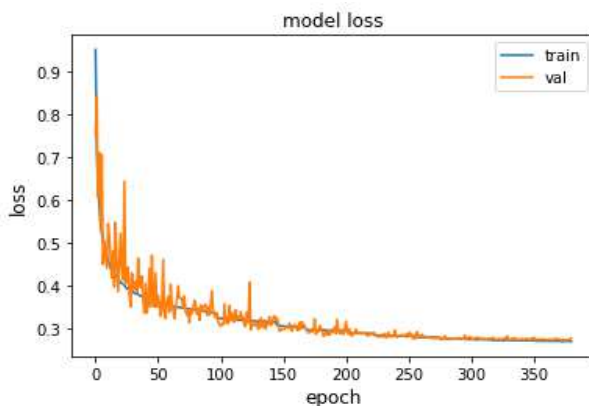


Fig 9. Loss curve for CNN model.

The 31 classes were tested with both CNN and Random Forest models. The models performed well with the test data. However, Random Forest was superior to CNN in terms of accuracy.

Table 1 depicts the comparison of the fabricated cf-rGO sensor with the previous reports. Our sensor was found to be superior in terms of quick response and high selectivity.

TABLE 1: Comparison of sensor performances

Sensor Type	Response (ppm)	Concentration	Response and recovery time	Ref.
RGO	930	400 ppm	31 s, 500 s	[24]
RGO	80	10 ppm	53 s, 554 s	[25]
RGO	12	800 ppm	505 s, 1340 s	[26]
RGO	23.2	50 ppm	41 s, 198 s	[27]
SnO ₂	190	800 ppm	36 s, 25 s	[27]
ZnO	180	800 ppm	48 s, 10 s	[27]
Cf-rGO	201	250 ppm	23 s, 71 s	This Work

VI. CONCLUSIONS

This research employs a single resistive sensor along with deep learning models to selectively detect ammonia within a complex gaseous mixture. The need for multiple sensors are eliminated through this study. The cf-rGO sensing layer was found to be highly selective towards ammonia along with strong immune behavior towards humidity interferences. At 500 ppm ammonia concentration, the sensor exhibited 275% response. Random forest and CNN was used to classify the different mixture of gases with an aim to detect ammonia in a binary or ternary mixture environment. Random forest with an accuracy of 96% dominates the CNN model (89% accuracy). Hence, we have successfully fabricated a functionalized sensor that can detect ammonia among various interferences. This method would also be helpful to accurately detect chronic kidney diseases.

REFERENCES

1. A. Sett, S. Dey, P. K. Guha, and T. K. Bhattacharyya, "ZnO/\$\gamma\$-Fe₂O₃ heterostructure toward high-performance acetone sensing." *IEEE Sensors Journal*, vol. 19, no. 19, pp. 8576-8582, 2019.
2. Young, Sheng-Joue, and Zheng-Dong Li, "Ethanol gas sensors composed of carbon nanotubes with Au nanoparticles adsorbed onto a flexible PI substrate." *ECS Journal of Solid State Science and Technology*, vol. 6, no. 10, pp. M130, 2017.
3. A. Sett, M. Mondal, and T. K. Bhattacharyya, "Hierarchical ZnO nanorods with tailored surface defects for enhanced acetone sensing." *IEEE Sensors Journal*, vol. 19, no. 10, pp. 3601-3608, 2019.
4. B. Olivier, "Ammonia toxicity to the brain: effects on creatine metabolism and transport and protective roles of creatine." *Molecular genetics and metabolism*, vol. 100, no. S53-S58, 2010.
5. K. Lokesh, G. Kavitha, E. Manikandan, G. K. Mani, K. Kaviyarasu, J. B. B. Rayappan, R. Ladchumananandasivam, J. S. Aanand, M. Jayachandran, and M. Maaiza, "Effective ammonia detection using n-ZnO/p-NiO heterostructured nanofibers." *IEEE Sensors Journal*, vol. 16, no. 8, pp. 2477-2483, 2016.
6. R. Ghosh, A. Midya, S. Santra, S. K. Ray, and P. K. Guha, "Chemically reduced graphene oxide for ammonia detection at room temperature." *ACS applied materials & interfaces*, vol. 5, no. 15, pp. 7599-7603, 2013.
7. R. S. Andre, L. A. Mercante, M. H. Facure, L. H. Mattoso, & D. S. Correa, "Enhanced and selective ammonia detection using In2O3/reduced graphene oxide hybrid nanofibers." *Applied Surface Science*, vol. 473 pp. 133-140, 2019.
8. J. A. Jarmoshti, A. Nikfarjam, H. Hajghassem, & S. M. Banihashemian, "Visible light enhancement of ammonia detection using silver nanoparticles decorated on reduced graphene oxide." *Mater. Res. Express*, vol. 6, no. 6, pp. 066306, 2019.
9. L. Xiong, M. He, C. Hu, Y. Hou, S. Han, & X. Tang, "Image presentation and effective classification of odor intensity levels using multi-channel electronic nose technology combined with GASF and CNN." *Sensors and Actuators B: Chemical*, vol. 395, pp. 134492, 2023.
10. S. Acharyya, B. Jana, S. Nag, G. Saha, and P. K. Guha, "Single resistive sensor for selective detection of multiple VOCs employing SnO₂ hollowspheres and machine learning algorithm: A proof of concept." *Sensors and Actuators B: Chemical*, vol. 321, pp. 128484, 2020.
11. T. Hayasaka, A. Lin, V. C. Copa, L. P. Lopez Jr, R. A. Loberternos, L. I. M. Ballesteros, Y. Kubota, Y. Liu, A. A. Salvador, and L. Lin,

"An electronic nose using a single graphene FET and machine learning for water, methanol, and ethanol." *Microsystems & nanoengineering*, vol. 6, no. 1, pp. 50, 2020.

12. J. Chu, W. Li, X. Yang, Y. Wu, D. Wang, A. Yang, H. Yuan, X. Wang, Y. Li, and M. Rong, "Identification of gas mixtures via sensor array combining with neural networks." *Sensors and Actuators B: Chemical*, vol. 329, pp.129090, 2021.
13. A. Sarkar, S. S. Hossain, and R. Sarkar, "Human activity recognition from sensor data using spatial attention-aided CNN with genetic algorithm." *Neural Computing and Applications*, vol. 35, no. 7, pp. 5165-5191, 2023.
14. D. R. Wijaya, F. Afianti, A. Arifianto, D. Rahmawati, and V. S. Kodogiannis, "Ensemble machine learning approach for electronic nose signal processing." *Sensing and Bio-Sensing Research*, vol. 36, pp. 100495, 2022.
15. H. Sundgren, F. Winquist, I. Lukkari, and I. Lundstrom, "Artificial neural networks and gas sensor arrays: quantification of individual components in a gas mixture." *Measurement Science and Technology*, vol. 2, no. 5, pp. 464, 1991.
16. L. Sarkar, A. Sett, S. Majumdar, and T. K. Bhattacharyya, "Reduced Graphene-Oxide-Based Silk-FET: A Facile Platform for Low Power and Room Temperature Detection of Formaldehyde." *IEEE Transactions on Electron Devices*, 2023.
17. A. Nandi, S. Majumdar, S. K. Datta, H. Saha, and S. M. Hossain, "Optical and electrical effects of thin reduced graphene oxide layers on textured wafer-based c-Si solar cells for enhanced performance." *Journal of Materials Chemistry C*, vol. 5, no. 8, pp. 1920-1934, 2017.
18. A. Sett, L. Sarkar, S. Majumdar, and T. K. Bhattacharyya, "Amplification of ammonia sensing performance through gate induced carrier modulation in Cu-rGO Silk-FET." *Scientific Reports*, vol. 13, no. 1, pp. 8159, 2023.
19. D. Panda, A. Nandi, S. K. Datta, H. Saha, and S. Majumdar, "Selective detection of carbon monoxide (CO) gas by reduced graphene oxide (rGO) at room temperature." *RSC advances*, vol. 6, no. 53, pp. 47337-47348, 2016.
20. J. Nilsson, A. C. Neto, F. Guinea, & N. M. R. Peres, "Electronic properties of graphene multilayers." *Physical review letters*, vol. 97, no. 26, pp. 266801, 2006.
21. Y. Peng, and J. Li, "Ammonia adsorption on graphene and graphene oxide: a first-principles study." *Frontiers of Environmental Science & Engineering*, vol. 7, pp. 403-411, 2013.
22. Y. Peng and J. Li, "Ammonia adsorption on graphene and graphene oxide: A first-principles study", *Frontiers Environ. Sci. Eng.*, vol. 7, no. 3, pp. 403-411, Jun. 2013.
23. Y. Xu, R. Meng, and X. Zhao, "Research on a gas concentration prediction algorithm based on stacking." *Sensors*, vol. 21, no. 5, pp. 1597, 2021.
24. Ghosh, R., Singh, A., Santra, S., Ray, S.K., Chandra, A. and Guha, P.K., "Highly sensitive large-area multi-layered graphene-based flexible ammonia sensor", *Sensors and Actuators B: Chemical*, 205, pp.67-73, 2014.
25. Andre, R.S., Mercante, L.A., Facure, M.H., Mattoso, L.H. and Correa, D.S, "Enhanced and selective ammonia detection using In₂O₃/reduced graphene oxide hybrid nanofibers" *Applied Surface Science*, 473, pp.133-140.
26. Sakthivel, B. and Nammalvar, G., "Selective ammonia sensor based on copper oxide/reduced graphene oxide nanocomposite", *Journal of Alloys and Compounds*, 788, pp.422-428, 2019.
27. Rout, C.S., Hegde, M., Govindaraj, A. and Rao, C.N.R., "Ammonia sensors based on metal oxide nanostructures", *Nanotechnology*, 18(20), p.205504, 2007.